Reactions on cell membranes: Comparison of continuum theory and Brownian dynamics simulations

Michael I. Monine and Jason M. Haugh[a)]

Department of Chemical and Biomolecular Engineering, North Carolina State University, Box 7905, 911 Partners Way, Raleigh, North Carolina 27695-7905

Biochemical transduction of signals received by living cells typically involves molecular interactions and enzyme-mediated reactions at the cell membrane, a problem that is analogous to reacting species on a catalyst surface or interface. We have developed an efficient Brownian dynamics algorithm that is especially suited for such systems and have compared the simulation results with various continuum theories through prediction of effective enzymatic rate constant values. We specifically consider reaction versus diffusion limitation, the effect of increasing enzyme density, and the spontaneous membrane association/dissociation of enzyme molecules. In all cases, we find the theory and simulations to be in quantitative agreement. This algorithm may be readily adapted for the stochastic simulation of more complex cell signaling systems. © *2005 American Institute of Physics.* [DOI: 10.1063/1.2000236]

I. INTRODUCTION

Reaction-diffusion problems on surfaces are encountered in a host of systems, most notably heterogeneous catalysis. Adam and Delbrück[1] first surmised that certain biological processes were aided by the reduction in dimensionality associated with adsorption to a surface, and the theory of diffusion-controlled reactions on planar surfaces has since been considered extensively in the chemical physics and biophysics literature.[2–15] A key aspect of diffusion-controlled reactions is the formation of a reactant depletion zone in the vicinity of an absorber, which limits the reaction rate.

In living cells, most biochemical pathways that transduce extracellular signals contain at least one critical reaction involving molecules residing in the inner leaflet of the plasma membrane, and such reactions are generally catalyzed by an enzyme that is activated at or recruited to the membrane. A distinguishing characteristic of such systems not encountered in traditional catalysis is the transient nature, or gating, of the enzyme activity at the membrane. A well-studied example is that of hormone receptors, which are activated by ligand binding and in turn catalyze the activation of membrane-anchored G-proteins. Linderman and co-workers have analyzed the dynamics of this system[16–18] and reversible, diffusion-controlled reactions in membranes more generally[13,19,20] using lattice Monte Carlo (LMC) simulations. These studies demonstrated that receptors that remain ligated for only a short time activate G-proteins more efficiently, because the reactant depletion zone will initially exhibit a sharp concentration gradient, whereas stable receptor-ligand complexes see the steady-state reactant profile for most of the time.

Although these models were applied to G-protein-coupled receptor signaling, the concept of enzyme activation and modification of membrane-associated substrates is encountered in signaling through many other classes of receptors. In systems where the relevant enzymes are recruited from the cell cytoplasm, as with growth factor and cytokine receptors, the concentrating effect of enzyme confinement at the membrane is sufficient for the enhancement of the reaction rate, which may (or may not) push the reaction into the diffusion-controlled regime.[21–23]

A continuum theory appropriate for a variety of signal transduction reactions in cell membranes was recently offered by one of us,[24] and in this theory the enzyme lifetime was modeled explicitly. The collision-coupling mechanism [Fig. 1(a)], first considered in the context of G-protein activation,[25] was used as a test case because it had been analyzed using LMC simulations.[13] The agreement with those simulations was found to be poor, however, as the continuum theory predicted significantly higher average reaction rates. The lack of agreement was attributed to the limited spatial resolution of LMC simulations of interacting point particles (as was the case with the data used for comparison), which would tend to underestimate the sharpness of the concentration gradients.

In this work, we have developed a Brownian dynamics (BD) algorithm useful for the simulations of interactions and reactions on cell membranes or other planar surfaces, under partial or complete diffusion control. As with all stochastic simulation approaches, enzyme gating is readily incorporated, and so we have revisited the collision-coupling mechanism with finite enzyme lifetimes. After reviewing the continuum theory in Sec. II, we outline our BD algorithm in detail in Sec. III. In Sec. IV, simulation results are compared with the theory, and we show that they are in excellent quantitative agreement.

[a)]Author to whom correspondence should be addressed; Fax: (919) 515-3465; electronic mail: jason_haugh@ncsu.edu
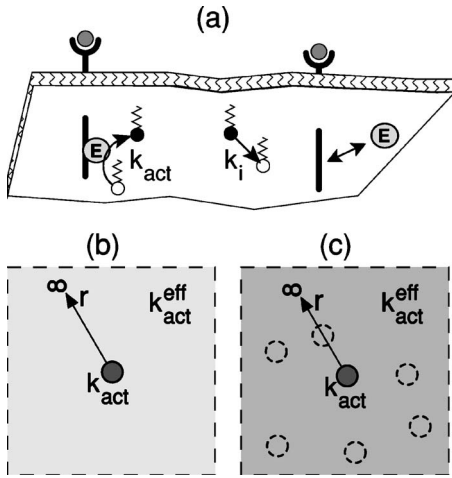
123, 074908-1

FIG. 1. Model and theory schematics. (a) Activation of the membrane-anchored substrate is enhanced by membrane-associated enzyme molecules (E), which act upon inactive substrate with second-order rate constant k_{act}. Substrate inactivation occurs with first-order rate constant k_i. The finite lifetime of the enzyme at the membrane is considered. (b) Dilute enzyme limit. The model considers only one enzyme on the membrane, and the density of activated substrate falls to approximately zero far away from the enzyme. The influence of substrate depletion in the vicinity of the enzyme is inferred from the value of k_{act}^{eff}, the effective enzymatic rate constant [Eq. (1)]. (c) High-density approximation. The model implicitly takes into account the influence of neighboring enzyme molecules, whose activities are homogenized using a mean-field theory.

II. THEORY

A. Effective enzymatic rate constant

The system of interest is illustrated in Fig. 1(a). An enzyme molecule, approximated as a uniformly reactive disk of radius s, associates with the membrane and catalyzes the conversion of a membrane-associated substrate from its inactive state to its active form with second-order rate constant k_{act}. Alternatively, s may be considered the sum of the two associating molecules' radii. The substrate reverts to its inactive state spontaneously, with first-order rate constant k_i. The constant area density of total substrate, inactive and active, is defined as n_{tot}, and both species diffuse laterally with diffusion coefficient D relative to the enzyme. It is noteworthy that this problem is physically distinct yet mathematically identical to that of reaction by surface diffusion on a catalyst with adsorption and desorption of reactant from the gas phase.[5]

Defining r as the radial distance from the center of the enzyme and n_i as the density of substrate in the inactive state, the catalytic action of the enzyme is modeled by imposing a Collins-Kimball radiation boundary condition at $r = s$; the reaction rate is also posed in terms of an effective rate constant, defined as k_{act}^{eff},

$$2\pi s D \left. \frac{\partial n_i(r,t)}{\partial r} \right|_{r=s} = k_{act} n_i(s,t) = k_{act}^{eff}\langle n_i \rangle, \tag{1}$$

where $\langle n_i \rangle$ is the average inactive substrate density in the membrane. The value of k_{act}^{eff} is used to implicitly assess the influence of spatial effects on the reaction rate in the entire membrane. Equation (1) is nondimensionalized as follows:

$$2\pi \left. \frac{\partial \Psi(\rho,\tau)}{\partial \rho} \right|_{\rho=1} = \kappa \Psi(1,\tau) = \alpha\langle\Psi\rangle, \tag{2}$$

where $\Psi = n_i/n_{tot}$, $\tau = Dt/s^2$, $\rho = r/s$, $\kappa = k_{act}/D$, and $\alpha = k_{act}^{eff}/D$. The quantity we wish to derive is α, the dimensionless effective enzymatic rate constant.

When an enzyme molecule spends a long time at the membrane, a constant substrate profile $\Psi_{ss}(\rho)$ is established around it, and the enzymatic rate is characterized by a steady-state value of α,

$$\alpha_\infty = \kappa \frac{\Psi_{ss}(1)}{\langle\Psi\rangle}, \tag{3}$$

where α_∞ denotes the effective rate constant in the limit of infinite enzyme lifetime at the membrane. In general, the enzyme may dissociate or otherwise "switch off" before the substrate concentration can achieve the steady-state profile. In relation to catalysis, this problem is analogous to that of two reacting molecules that adsorb transiently to the catalyst, where they react through surface diffusion. To account for enzymatic activity within a finite time interval τ_{on}, Eq. (3) may be rewritten as suggested previously,[24]

$$\alpha = \kappa \frac{\int_0^{\tau_{on}} \Psi(1,\tau)d\tau}{\langle\Psi\rangle\tau_{on}}. \tag{4}$$

Equation (4) describes only the transient behavior, however, when considering the effective rate constant averaged over all enzyme recruitment events. If we consider the dissociation or deactivation of the enzyme as a random, first-order process and define τ_{on} as the mean lifetime of the enzyme-on state, the probability of an enzyme remaining active after time τ is $P_{on}(\tau) = \exp(-\tau/\tau_{on})$. Thus, averaging over many enzyme recruitment events, we obtain

$$\alpha = \kappa \frac{\int_0^\infty \Psi(1,\tau)P_{on}(\tau)d\tau}{\langle\Psi\rangle\int_0^\infty P_{on}(\tau)d\tau} = \kappa \frac{\int_0^\infty \Psi(1,\tau)e^{-\tau/\tau_{on}}d\tau}{\langle\Psi\rangle\tau_{on}}. \tag{5}$$

B. Dilute enzyme limit

The dilute enzyme limit requires that enzymes at the membrane are sparse [Fig. 1(b)]. The density of substrate in the inactive state is conserved by

$$\frac{\partial\Psi}{\partial\tau} = \nabla_\rho^2\Psi + \text{Da}(1 - \Psi). \tag{6}$$

The dimensionless parameter Da ($\text{Da} = k_i s^2/D$) is a Damköhler number comparing the rates of inactivation and diffusion of the substrate. Far away from each enzyme molecule, all of the substrate is inactive,

$$\left. \frac{\partial\Psi}{\partial\rho} \right|_{\rho\to\infty} = 0, \quad \Psi|_{\rho\to\infty} = 1. \tag{7}$$

Moreover, the gradient of the substrate density is sharp and localized around the enzyme boundary and, therefore,

$\langle\Psi\rangle = \Psi|_{\rho\to\infty} = 1$. Together with Eq. (2), the steady-state solution of Eq. (6) is obtained,

$$\Psi_{ss}(\rho) = 1 - \frac{\kappa K_0(\mathrm{Da}^{1/2}\rho)}{2\pi\mathrm{Da}^{1/2}K_1(\mathrm{Da}^{1/2}) + \kappa K_0(\mathrm{Da}^{1/2})}, \qquad (8)$$

$$\alpha_\infty = \frac{2\pi\kappa\mathrm{Da}^{1/2}K_1(\mathrm{Da}^{1/2})}{2\pi\mathrm{Da}^{1/2}K_1(\mathrm{Da}^{1/2}) + \kappa K_0(\mathrm{Da}^{1/2})}, \qquad (9)$$

where K_m are modified Bessel functions of order m. The result in Eq. (9) is well known from the models of analogous systems.[5,9,14]

In this limit, we may also assume that $\Psi(\rho,0) = 1$ initially, and the transient solution follows from Eq. (6),

$$\Psi(\rho,\tau) = \Psi_{ss}(\rho) + \int_0^\infty \frac{\kappa\Phi(1)\Phi(\rho)e^{-(\lambda^2+\mathrm{Da})\tau}\lambda\,d\lambda}{2\pi(\lambda^2+\mathrm{Da})(1+g^2(\lambda))},$$

$$\Phi(\rho) = J_0(\lambda\rho) - g(\lambda)Y_0(\lambda\rho), \qquad (10)$$

$$g(\lambda) = \frac{\kappa J_0(\lambda) + 2\pi\lambda J_1(\lambda)}{\kappa Y_0(\lambda) + 2\pi\lambda Y_1(\lambda)},$$

where $\Psi_{ss}(\rho)$ is the steady-state substrate profile in the infinite lifetime limit from Eq. (8), and J_m and Y_m are Bessel functions of order m. Incorporating Eqs. (5) and (8)–(10) and simplifying, we derive

$$\alpha = \alpha_\infty + \frac{8}{\pi}\int_0^\infty \frac{h(\lambda)d\lambda}{(\lambda^2+\mathrm{Da})[1+\tau_{on}(\lambda^2+\mathrm{Da})]},$$

$$\qquad (11)$$

$$h(\lambda)$$

$$= \frac{\lambda}{[J_0(\lambda)+(2\pi\lambda/\kappa)J_1(\lambda)]^2 + [Y_0(\lambda)+(2\pi\lambda/\kappa)Y_1(\lambda)]^2}.$$

C. High-density approximation

When enzymes are not necessarily dilute and dispersed randomly in the membrane, one can approximate the influence of neighboring enzymes by smearing out their action in the bulk [Fig. 1(c)].[24] Taking n_E as the enzyme density at the membrane, Eq. (6) is altered to give

$$\frac{\partial\Psi}{\partial\tau} = \nabla_\rho^2\Psi + \mathrm{Da}(1-\Psi) - \alpha\eta_E\Psi,$$

$$\qquad (12)$$

$$\eta_E = n_E s^2.$$

The average substrate density some distance away from the enzyme molecule of interest approaches $\langle\Psi\rangle = \mathrm{Da}/(\mathrm{Da} + \alpha\eta_E)$, and hence with a rescaling of variables, Eq. (12) takes the form of Eq. (6) written for $\Psi^* = \Psi/\langle\Psi\rangle$ and $\mathrm{Da}^* = \mathrm{Da} + \alpha\eta_E$. The effective rate constant α is solved implicitly following the simple substitution of Da^* for Da in Eqs. (9) and (11).

III. BROWNIAN DYNAMICS MODEL

Our BD model is based on the following assumptions: (i) all membrane-associated processes are modeled in planar
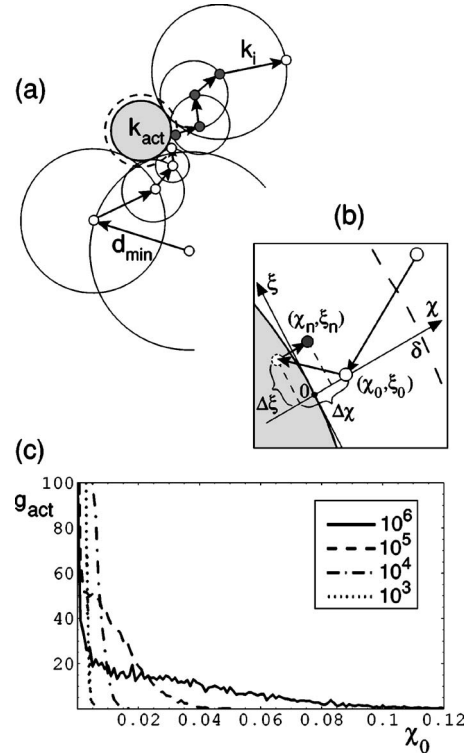

FIG. 2. Brownian dynamics algorithm. (a) In the bulk membrane, the next position of the particle is taken to be random on the concentric circle boundary touching the closest enzyme (shown by a gray disk). An inactive particle (shown by a small open circle) can be activated in a thin *activation layer* next to the enzyme boundary. The activated particle (shown by a small filled circle) is converted back to the inactive state while making diffusion steps. (b) In the activation layer, a new rectangular coordinate system χ, ξ is defined, neglecting curvature of the boundary (the size of the activation layer and thus the curvature is exaggerated here for the purpose of illustration). The next particle position (χ_n, ξ_n) is defined by displacements $\Delta\chi, \Delta\xi$ sampled from the Gaussian distribution and assuming that the enzyme boundary is reflective. Particle activation is modeled as a one-dimensional problem in χ. (c) Distribution density function g_{act} describing the number of activation events (with $\kappa = 10^6$) as a function of the initial distance to the reactive boundary, with $s = 3.5$ nm and $\Delta t_{AL} = 10^{-9}$ s. The varied parameter is D (in nm^2/s).

geometry, (ii) enzyme molecules are approximated by disks of radius s, while substrate molecules are modeled as point particles that do not interact with each other (this is equivalent to considering s to be the sum of the enzyme and substrate radii), and (iii) the active and inactive substrate particles diffuse laterally with the same isotropic diffusion coefficient D relative to the (immobile) enzymes. The BD algorithm, illustrated in Fig. 2, uses an adaptive time step (Δt) and distinguishes between two regions of the cellular membrane: bulk membrane, where long-distance steps are considered, and a so-called *activation layer* surrounding each enzyme, where the substrate particles make short-distance steps and the activation reaction is considered. The size of the thin activation layer is characterized by thickness $\delta \ll s$. Particle inactivation occurs with probability $P_i = 1 - \exp(-k_i\Delta t)$ within both the bulk and activation layer regions. The model assumes periodic boundary conditions at the edges of the simulation box.

In the bulk membrane, a particle is advanced according to the first-passage-time method.[26–28] The next position of the particle is chosen to be uniformly distributed on the

boundary of a circle centered on the current position of the particle. The radius of this circle is usually chosen to be equal to the distance to the closest reactive boundary, d_{min}, and the time required for this step is determined as $\Delta t = d_{min}^2/4D$ [Fig. 2(a)]. In certain cases, however, this algorithm tends to underpredict the frequency of collisions between the particle and reactive boundary, as a particle will often travel a path that is farther than d_{min} during the time step. This was found to be the case when enzymes dissociate rapidly ($t_{on} < \langle d \rangle^2/4D$, $\tau_{on} \ll 1/\eta_E$, with $\langle d \rangle$ denoting an average half-distance between enzymes), and so in these situations a finer time discretization was introduced in our algorithm by choosing

$$\Delta t = \min\left\{\frac{d_{min}^2}{4D}, \nu t_{on}, \frac{1}{k_i}\right\}, \tag{13}$$

where $\nu \sim 10^{-3} - 10^{-2}$.

For any particle reaching the activation layer, a new rectangular coordinate system χ, ξ is defined with the χ direction perpendicular to the enzyme boundary [Fig. 2(b)], and all particles in the system are subsequently sampled with a sufficiently short constant time step Δt_{AL}; particle displacements $\Delta \chi$ and $\Delta \xi$ are sampled as Gaussian variables with standard deviations equal to $(2D\Delta t_{AL})^{1/2} \ll \delta$. The reactive boundary is reflective, and so a new coordinate χ_n along the normal to the boundary is defined as $\chi_n = |\chi_0 + \Delta \chi|$, whereas $\xi_n = \xi_0 + \Delta \xi$. The particle coordinates (χ_n, ξ_n) are then mapped to (x_n, y_n). Transition from the inactive state to the active one is modeled as described previously,[28] with activation taking place if

$$\frac{p_A(\chi_n, \chi_0, \Delta t_{AL})}{p_R(\chi_n, \chi_0, \Delta t_{AL})} \le z, \tag{14}$$

where z is a random number drawn uniformly in the range (0,1), and p_A and p_R are the well-known one-dimensional reaction (activation) and reflection propagators.[29,30] The one-dimensional approximation is justified here because, by design, $\delta \ll s$.

The considerations above constrain the choice of the simulation parameters δ and Δt_{AL}. Further, while the ratio $D\Delta t_{AL}/\delta^2$ must be sufficiently small to ensure accuracy, the computation time increases as this ratio shrinks. Given this trade-off, we analyzed the distribution density function, g_{act} [Fig. 2(c)]; discrete values of the number of activation events, $N_{act}(\chi_0)$, in a given time step from starting positions χ_0 are normalized such that integration of g_{act} over χ_0 gives 1,

$$g_{act}(\chi_0) = N_{act}(\chi_0) \left/ \int_0^\infty N_{act}(\chi')d\chi' \right. . \tag{15}$$

A high value of κ was used here ($\kappa = 10^6$), such that an activation event implies that a collision with the reactive boundary occurred. For a given time step, the probability of activation from $\chi_0 = \delta$ should be low, and thus we found an appropriate time step Δt_{AL} (10^{-9} s) and activation layer thickness δ [0.05 or 0.1 nm; Fig. 2(c)].

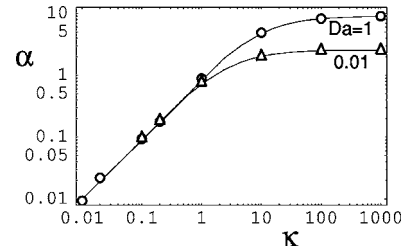The efficiency of the BD algorithm is significantly enhanced by assuming that the substrate particles do not

FIG. 3. Comparison of theory and BD simulation results: long-lived enzymes at low densities. The effective enzymatic rate constant ($\alpha = k_{act}^{eff}/D$) is shown as a function of the true reaction rate constant ($\kappa = k_{act}/D$). Da is the scaled inactivation rate constant ($Da = k_i s^2/D$). The dilute enzyme limit [Eq. (9)] is shown by the solid curves; simulation results are represented by the symbols. Simulations were performed for a periodic domain with one enzyme at sufficiently low densities ($\eta_E = n_E s^2 = 10^{-5} \ll Da$).

interact with each other, because we need not perform simulations for an array of particles. The time step is determined by the particle with the smallest Δt, and so it is more efficient to simulate one particle at a time and perform a finite number of independent simulations equal to the total number of particles, N_{part} (10^4 was found to be suitable). The effective rate constant in the BD model is evaluated as

$$\alpha = \frac{N_{act}A}{\langle N_i \rangle \langle N_E \rangle t_{sim}D}, \tag{16}$$

where N_{act} is the total number of substrate activation events, A is the area of membrane simulated, and $\langle N_i \rangle$ and $\langle N_E \rangle$ are average numbers of inactive substrate particles and active, membrane-localized enzyme molecules, respectively (obtained by averaging over the total simulation time t_{sim}). Equation (16) is a discrete analog of the integral expression used in the continuum theory [Eq. (5)].

In simulations with dissociating enzyme complexes, the finite lifetime of the ith on-state for the jth enzyme is sampled as $t_{on,ij} = -t_{on} \ln(1-z_{ij})$, where z_{ij} is a random number drawn uniformly in the range (0,1). The duration of each enzyme-off state, where applicable, is determined in the same fashion.

IV. RESULTS AND DISCUSSION

A. Simulations of enzymes with infinite lifetime at the membrane

In our first set of simulations, we assessed the simple case of a single, fixed enzyme in the membrane with infinite lifetime (Fig. 3). The size of the simulation box was such that the low-density approximation was valid, and BD simulations were run until a steady-state value of the effective enzymatic rate constant α was reached [Eq. (16)]. The exact analytical solution in this case [Eq. (9)] predicts a dependence on two dimensionless parameters: Da ($Da = k_i s^2/D$) and κ ($\kappa = k_{act}/D$). The simulation results are in agreement with the theory, which predicts that the diffusion-limited value of α is reached for large κ; this plateau value is a positive function of Da, as the inactivation process sharpens the gradient while reducing the size of the depletion zone surrounding the enzyme (Fig. 3). It was confirmed that these
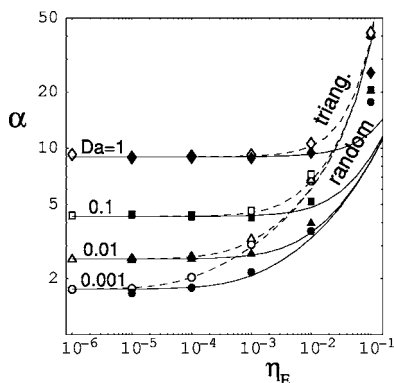
FIG. 4. Evaluation of the mean-field approximation for higher enzyme densities. The effective enzymatic rate constant is shown as a function of enzyme density ($\eta_E = n_E s^2$) in the diffusion limit ($\kappa = 10^6$). The solid curves are the theoretical predictions [Eq. (9), with $\mathrm{Da}^* = \mathrm{Da} + \alpha \eta_E$ substituted for Da]; simulation results, with a random array of 200 enzymes, are represented by the filled symbols. Theory and simulation results for regular enzyme arrays, arranged on a triangular lattice, are represented by the dashed curves and open symbols, respectively.
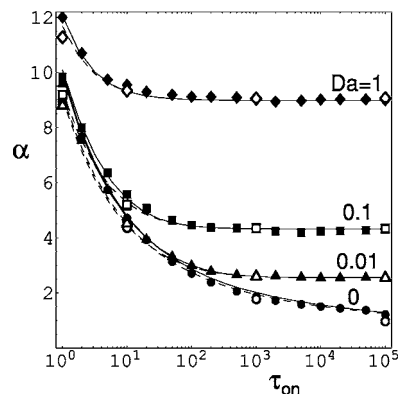

FIG. 5. Comparison of theory and simulation results: single enzyme with finite lifetime. The effective enzymatic rate constant was computed as a function of the mean lifetime of the enzyme on the membrane, $\tau_{\mathrm{on}} = D t_{\mathrm{on}}/s^2$, in the diffusion-limited regime ($\kappa = 10^6$) and at low enzyme densities ($\eta_E = 10^{-5}$). The transient solution given by Eq. (4) (Ref. 24) and BD simulation results with deterministic enzyme lifetimes are shown by the solid curves and closed symbols, respectively. The probabilistic lifetime solution given by Eq. (11) and corresponding BD results are shown by the dashed curves and open symbols, respectively.

simulation results do not depend on the choices of D and s, as long as the activation layer thickness and time step are set accordingly [Fig. 2(c)].

The effect of increasing the enzyme density, in the limit of fast reaction ($\kappa = 10^6$) and again with long-lived enzymes at the membrane, was evaluated next (Fig. 4). The simulation box was populated with a total of 200 randomly placed enzyme disks; the area of the simulation box A was determined from the prescribed enzyme density. The simulation results show good agreement with the implicit high-density approximation [Eq. (9), with $\mathrm{Da}^* = \mathrm{Da} + \alpha \eta_E$ substituted for Da] for enzyme densities of $\eta_E \sim 10^{-2}$ and below. At higher densities ($\eta_E \sim 0.1$, or an area fraction ~ 0.3), outside the physiological range, the approximation breaks down as presumed previously[24] (Fig. 4). We also compared the BD model for the case of enzymes arranged in a regular array. These test simulations were performed with a single enzyme at the center of a rhombic unit cell with periodic boundary conditions, representing a triangular lattice, and the results were compared with the previously derived exact analytical solution for a circular cell [with reflection boundary condition at radius $r = (\pi n_E)^{-1/2}$].[5,7] As expected, the agreement was good for the entire range of enzyme densities tested (Fig. 4). Both the mean-field theory and BD model predict that the dilute enzyme limit result is achieved at sufficiently low values of η_E, regardless of lattice configuration, and that the effective enzymatic reaction rate becomes insensitive to Da at high enzyme densities.

B. Simulations of enzymes with finite lifetime at the membrane

The theory and BD model were extended to account for the kinetics of enzyme activation/deactivation (or its membrane association/dissociation). Before considering the problem involving an array of unstable enzymes, the transient action of a single enzyme molecule upon the surrounding substrate particles was examined in the low-density, fast reaction limit ($\eta_E = 10^{-5}$, $\kappa = 10^6$; Fig. 5). The

effective enzymatic rate constant was determined as a function of the dimensionless enzyme lifetime, τ_{on} ($\tau_{\mathrm{on}} = D t_{\mathrm{on}}/s^2$), with specified values of Da. Theoretical predictions in the dilute enzyme limit considered both deterministic [the enzyme is on for a specified time t_{on}; Eq. (4) (Ref. 24)] and probabilistic [Eqs. (5) and (11)] lifetimes of the enzyme activity, and corresponding BD simulations were performed. In the case of probabilistic lifetimes, the BD algorithm was repeated for many sampled values of t_{on}, and values of α were calculated using aggregate values of N_{act}, t_{sim}, and $\langle N_i \rangle$ in Eq. (16). In all cases, we found good agreement between theory and BD results and only a subtle difference between deterministic and probabilistic enzyme lifetimes (Fig. 5). The transient behavior is more prolonged when the enzymatic reaction is limited by relatively slow inactivation of the substrate (low Da).

Finally we show that the continuum theory can approximate the effective enzymatic rate constant in the realistic system consisting of an array of enzymes that associate and dissociate spontaneously (Fig. 6). Such a system was considered previously by Shea et al.,[13] who used LMC simulations to obtain effective rate constants for receptor-associated enzyme activity activated by external ligand binding. The average lifetime of the enzyme was thus determined by the dissociation rate constant of the ligand, k_r ($t_{\mathrm{on}} = k_r^{-1}$), and the average duration between ligand-binding events for each receptor, t_{off}, was determined by the external ligand concentration; in those simulations, k_r (and thus t_{on}) was varied while keeping the ratio $t_{\mathrm{off}}/t_{\mathrm{on}}$ (and thus the average active enzyme density, η_E) constant, and it was reasoned that t_{off} would be large enough such that the surrounding substrate would be inactivated prior to the next ligand-binding event.[24] The BD algorithm was run for a random array of 200 receptors, with the enzyme activation state of each tested at specified time intervals ($10^{-2} t_{\mathrm{on}}$), and a running average of α was computed [Fig. 6(a)]. The steady-state value of α (determined at $t_{\mathrm{sim}} = 10^3 t_{\mathrm{on}}$) was compared with the continuum
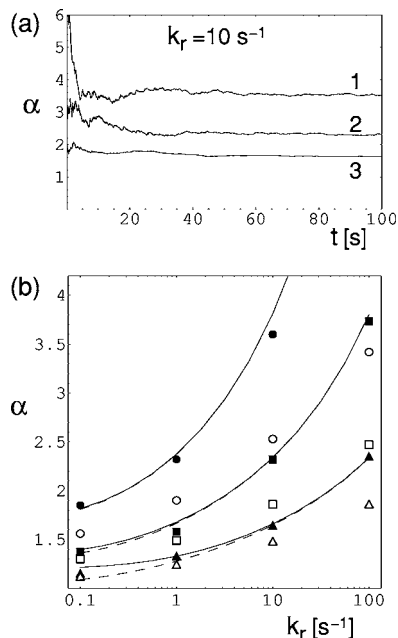
FIG. 6. Random receptor array with spontaneous enzyme association/dissociation. Constant parameter values are taken from Shea et al. (Ref. 13): $k_i = 0.1$ s^{-1}, $s = 3.5$ nm, and $\eta_E = 2.333 \times 10^{-5}$; $k_r = 1/t_{on}$ is the dissociation rate constant of the enzyme, and conditions are such that the duration of the enzyme-off state is $t_{off} = 20 t_{on}$. BD computations were performed for a random array of 200 receptors with spontaneous association and dissociation of enzymes. (a) Relaxation of α toward steady-state behavior in long-run BD simulations. The relative diffusion coefficient D is varied as (1) 2×10^{-11}, (2) 2×10^{-10}, or (3) 2×10^{-9} cm^2/s. (b) Effective rate constant as a function of k_r. The closed symbols denote BD results (averaged over the fluctuations in the steady-state regime), and the open symbols denote values reported by Shea et al. (Ref. 13 and 31): circles, $D = 2 \times 10^{-11}$; squares, $D = 2 \times 10^{-10}$; and triangles, $D = 2 \times 10^{-9}$. The solid curves show the mean-field theory predictions (accounting for the enzyme density), and the dashed curves show the dilute enzyme limit given by Eq. (11).

theory and LMC results; as observed previously, the theory and LMC predictions do not agree, yet our BD results are in good agreement with theory for the same parameter values used by Shea et al. [Fig. 6(b)].

The discrepancies in the LMC simulations apparently stem from an inability to resolve off-lattice events.[24] Accordingly, the deviations are largest when substrate gradients in the vicinity of the enzyme are steep (low D and high k_r), and Shea et al. acknowledged that there is a maximum value of α that could be obtained in their simulations of point particles, set by the frequency of bimolecular collisions on a lattice $(\alpha = 4)$.[6] It is expected that this resolution issue is relaxed when either of the interacting particles fills several nodes, with a defined reaction boundary, as implemented in more recent LMC simulations of membrane interactions.[20]

V. CONCLUSIONS

We have developed a Brownian dynamics algorithm that is suitable for stochastic simulation of reactions and interactions on surfaces, which we aim to apply to systems that involve the assembly of signaling complexes and resulting enzymatic reactions at cell membranes. To validate the BD algorithm, we have simulated the collision-coupling mechanism of enzyme action and compared the results with both exact (dilute enzyme limit) and approximate (mean-field treatment of neighboring enzymes) theoretical predictions, with full accounting of finite enzyme lifetimes. Close quantitative agreement was seen in all cases, and we found that the mean-field approximation is valid unless the enzyme density exceeds previously prescribed limits. Finally, we conclude that lattice Monte Carlo simulations of point particles systematically underestimate the reaction rate because of an inability to resolve sharp gradients, a problem that is likely to be alleviated when each particle has a defined area comprised of many nodes.

[1] G. Adam and M. Delbrück, in *Structural Chemistry and Molecular Biology*, edited by A. Rich and N. Davidson (Freeman, San Francisco, 1968), pp. 198–215.
[2] K. R. Naqvi, Chem. Phys. Lett. **28**, 280 (1974).
[3] H. C. Berg and E. M. Purcell, Biophys. J. **20**, 193 (1977).
[4] F. W. Wiegel and C. DeLisi, Am. J. Physiol. **12**, R475 (1982).
[5] D. L. Freeman and J. D. Doll, J. Chem. Phys. **78**, 6002 (1983).
[6] D. C. Torney and H. M. McConnell, Proc. R. Soc. London, Ser. A **387**, 147 (1983).
[7] B. Goldstein, R. Griego, and C. Wofsy, Biophys. J. **46**, 573 (1984).
[8] J. Keizer, J. Ramirez, and E. Peacock-Lopez, Biophys. J. **47**, 79 (1985).
[9] B. Goldstein, C. Wofsy, and H. Echavarria-Heras, Biophys. J. **53**, 405 (1988).
[10] D. V. Khakhar and U. S. Agarwal, J. Chem. Phys. **99**, 9237 (1993).
[11] P. B. Gaspers, A. P. Gast, and C. R. Robertson, J. Colloid Interface Sci. **172**, 518 (1995).
[12] A. Molski, S. Bergling, and J. Keizer, J. Phys. Chem. **100**, 19049 (1996).
[13] L. D. Shea, G. M. Omann, and J. J. Linderman, Biophys. J. **73**, 2949 (1997).
[14] A. Molski, J. Phys. Chem. B **104**, 4532 (2000).
[15] H. Berry, Biophys. J. **83**, 1891 (2002).
[16] P. A. Mahama and J. L. Linderman, Biophys. J. **67**, 1345 (1994).
[17] P. J. Woolf and J. J. Linderman, Biophys. J. **84**, 3 (2003).
[18] H. L. Zhong, S. M. Wade, P. J. Woolf, J. J. Linderman, J. R. Traynor, and R. R. Neubig, J. Biol. Chem. **278**, 7278 (2003).
[19] L. D. Shea and J. J. Linderman, J. Theor. Biol. **191**, 249 (1998).
[20] P. J. Woolf and J. J. Linderman, Biophys. Chem. **104**, 217 (2003).
[21] B. Grasberger, A. P. Minton, C. DeLisi, and H. Metzger, Proc. Natl. Acad. Sci. U.S.A. **83**, 6258 (1986).
[22] S. McLaughlin and A. Aderem, Trends Biochem. Sci. **20**, 272 (1995).
[23] J. M. Haugh and D. A. Lauffenburger, Biophys. J. **72**, 2014 (1997).
[24] J. M. Haugh, Biophys. J. **82**, 591 (2002).
[25] A. M. Tolkovsky and A. Levitski, Biochemistry **17**, 3795 (1978).
[26] S. Torquato and I. C. Kim, Appl. Phys. Lett. **55**, 1847 (1989).
[27] L. H. Zheng and Y. C. Chiew, J. Chem. Phys. **90**, 322 (1989).
[28] L. Batsilas, A. M. Berezhkovskii, and S. Y. Shvartsman, Biophys. J. **85**, 3659 (2003).
[29] G. Lamm and K. Schulten, J. Chem. Phys. **75**, 365 (1981).
[30] G. Lamm and K. Schulten, J. Chem. Phys. **78**, 2713 (1983).
[31] L. D. Shea (personal communication).